World Academy of Science, Engineering and Technology
International Journal of Mechanical and Mechatronics Engineering
Vol:3, No:8, 2009

The shaping of a triangle steel plate into an equilateral vertical steel by finite-element modeling

Tsung-Chia Chen

***Abstract*—**The orthogonal processes to shape the triangle steel plate into a equilateral vertical steel are examined by an incremental elasto-plastic finite-element method based on an updated Lagrangian formulation. The highly non-linear problems due to the geometric changes, the inelastic constitutive behavior and the boundary conditions varied with deformation are taken into account in an incremental manner. On the contact boundary, a modified Coulomb friction mode is specially considered. A weighting factor *r*-minimum is employed to limit the step size of loading increment to linear relation. In particular, selective reduced integration was adopted to formulate the stiffness matrix. The simulated geometries of verticality could clearly demonstrate the vertical processes until unloading. A series of experiments and simulations were performed to validate the formulation in the theory, leading to the development of the computer codes. The whole deformation history and the distribution of stress, strain and thickness during the forming process were obtained by carefully considering the moving boundary condition in the finite-element method. Therefore, this modeling can be used for judging whether a equilateral vertical steel can be shaped successfully. The present work may be expected to improve the understanding of the formation of the equilateral vertical steel.

***Keywords*—**elasto-plastic, finite element, orthogonal pressing process, vertical steel.

I. Introduction

SHEET-metal pressing is one of the most frequently applied sheet forming operations. Although the process is simple, the pressing operation presents many technical problems of manufacturing. These include the prediction of spring-back after forming for tool design, control of the process, the accuracy of the component shape, fractures originating from the stretched surface, and the estimation of the punch load of the pressing in press selection.

The pressing process of equilateral vertical steel is pressing in a punch which has a orthogonal peak, so that the deformation shape follows from the punch's pressing the sheet into the die. After the pressing process is completed, the tools are removed and the sheet returns to its final shape after unloading, at which residual stresses are in equilibrium. The unloading after forming strongly influences the final shape of products. In precise components of pressing depends on process variables, including tensile properties and geometrical parameters. Consequently, the unloading state after forming in pressing is hard to estimate. The products are often used to provide additional support for connecting to components.

In this study, an elasto-plastic finite element computer code, based on an updated Lagrangian scheme, is adopted to simulate pressing processes efficiently. A special feature of the scheme is the selective reduced integration method [1], which has been proven to be efficiently applicable to nearly incompressible material. The method is used to treat the shell elements in the finite-element model. A modified Coulomb friction law was employed to treat the discontinuous alteration in the sliding-sticking state of friction at the contact interface. An extended *r*-minimum method was used to determine the dependence of the sheet-tool contact condition on deformation. The method is developed to describe the alternating sliding direction that occasionally increases computational difficulty. Some key parameters, e.g. the thickness distribution, stress distribution, fracture phenomena, and forming limitation of blanks, should be first obtained by numerical simulation for predicting whether the fracture conforms to a specific geometry, such as the punch fillet radius and the die fillet radius, before the dies are manufactured. This approach can save effort compared with the conventional trial-and-error approach in the factory. The numerical results of punch load, thickness variation and finished shape show good agreement with the results of experiment.

II. Description of the Basic Theory

A. Variational Principle

The updated Lagrangian formulation is based on the modified principle of virtual velocity [2]:

$$\int_V \{(\sigma_{ij}^J - 2\sigma_{ik}D_{ik})\delta D_{ij} + \sigma_{jk}L_{ik}\delta L_{ij}\}dV = \int_{S_t} \dot{f}_i \delta v_i dS \qquad (1)$$

where σ^J is the Jaumann derivative of Cauchy stress σ. L is the gradient of the velocity field ($L = \partial v / \partial x$); D and W are, respectively, the symmetric and anti-symmetric parts of L. The derivation of this equation considers the fact that, for sheet metal forming, $\det(\partial x / \partial x_0) \cong 1$. Hence, $\tau^J = \sigma^J$ where τ^J is the Jaumann derivative of the Kirchhoff stress. Constitutive equations can be defined as a small strain, linear elasticity and the large deformation, rate-independent, work-hardening plasticity [3]:

Tsung-Chia Chen is with the Mechanical Engineering Department, National Chin-Yi University of Technology, Taiping, Taichung County 411 Taiwan, R.O.C. (corresponding author to provide phone: +886-4-23924505ext7154; fax: +886-4-23930681; e-mail: ctchen@mail.ncut.edu.tw).

$$\sigma_{ij}^{J} = C_{ijkl}^{ep} D_{kl} = C_{ijkl}^{ep} L_{kl} \tag{2}$$

where C_{ijkl}^{ep} is the symmetric tangent constitutive matrix.

Substituting Eq. (2) into Eq. (1) yields the final form of the principle of virtual velocity:

$$\int_V \bar{C}_{ijkl} L_{kl} \delta L_{ij} dV = \int_{S_t} \dot{f}_i \delta v_i dS \tag{3}$$

where, $\bar{C}_{ijkl} = C_{ijkl}^{ep} + \Omega_{ijkl}$; $\Omega_{ijkl} = \frac{1}{2}\left(\sigma_{jl}\delta_{ik} - \sigma_{ik}\delta_{jl} - \sigma_{il}\delta_{jk} - \sigma_{jk}\delta_{il}\right)$.

B. Stiffness Equation

The aforementioned problem is solved in the standard way: Eq. (3) is integrated from time t to $t + \Delta t$, where Δt is a small time increment. All rate quantities are simply replaced by incremental quantities, assuming that rates are maintained constant in each incremental step. Standard finite element discretization, and the introduction of an elemental shape function enable Eq. (3) to be replaced by a system of algebraic equations,

$$K\Delta u = \Delta F + \Delta C \tag{4}$$

where K is the elastic-plastic stiffness matrix and Δu represents the nodal displacement increment. The terms ΔF and ΔC are taken from the right-hand side of Eq. (3). The stiffness matrix K is described at time t and is considered to be a constant within the time increment Δt. The so-called "*r*-minimum" method [4] is applied to limit the size of the time step.

C. Selective Reduced Integration Formulation

The volume of a plastic medium is incompressible. Therefore, implementing the full integration technique for finite elements leads to over-strong constraint on thin plates. This phenomenon is caused by setting to zero the shear strains γ_{xz} and γ_{yz} during deformation [5]. The selective reduced integration (SRI) procedure has been proven to treat effectively such problems as those involving volumetrically stiff contribution [6]. The generalized formulation of SRI due to Hughes [7] was used to develop the finite-element program in this study, which uses a four-node shell element.

III. Experimental Work

A. Experimental Material

The material data of the sheet steel, supplied by the China Steel, was tested according to ASTM E646-78 in the directions of 0°, 45° and 90° with respect to the rolling direction for calculations and experiments. The average values obtained are as follows: thickness, t = 1.0 mm; yield stress, σ_y = 247 MPa; stress-strain curve, $\bar{\sigma} = 649(0.04 + \bar{\varepsilon}_p)^{0.3}$ MPa; Poisson's ratio, ν = 0.3; Young's modulus, E = 210.0 GPa.

B. Experimental Equipment and Blank Shape

Pressing tests were carried out using a punch with a diameter of 65.3 mm and a die with a diameter of 112 mm. Figure 1 presents the dimensions of the tools used in the pressing process. The corner radii of the punch (Rp) and die (Rd) were 4.0 and 5.0 mm, respectively. Orthogonal pressing tests were performed in a 500ton mechanical press. The blank shape designed by trial-and-error was simply fabricated with an equivalent surface area to the final product, and then a size of final blank was determined through many experiments [8-9]. Figure 2 presents the blank shape designed by trial-and-error. Figure 3 present experimental results for successive process of orthogonal pressing. Measurement of the thickness distribution of the product has been made a point micrometer measuring from the center of the product to the outer edge, and the thickness of the product is measured in three vertical sides.

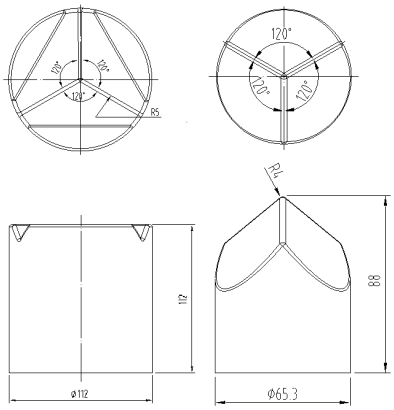

Fig. 1 Dimensions of the tools (mm) used in the pressing process

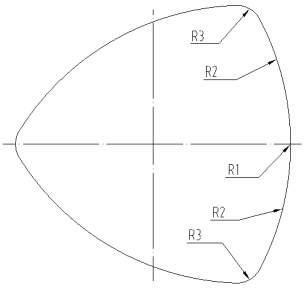

Fig. 2 Blank shape designed by trial-and-error

Fig. 3 Experimental result for successive process

IV. NUMERICAL ANALYSIS

This work used a four-node rectangular shell element to derive a stiffness matrix and employed CAD software. The established tool and blank were meshed and transferred into a data file. The elasto-plastic large deformation 3-D finite element method was used to perform numerical analysis. The simulated punch load and punch stroke were compared with the corresponding experiment results, and the results of the analysis were output to CAD software to show the deformation figure of stress and strain distribution. The above information can be used as a reference support designing a tool and its use in manufacturing.

In simulating orthogonal pressing processes, the finite element mesh of the tool is triangular elements. Figure 4(a) depicts the profile of the die and punch head. Figure 4(b) presents rectangular elements when the blanks are meshed. In simulating the blank, appropriate boundary conditions must be imposed. Conditions are set on the nodes such that the direction of rotation or displacement of nodes is constrained. In the simulation, the X-axis's nodes of the blank were constrained the displacement in the Y-direction. Additionally, the central node of the blank were constrained the displacement in the X-direction and Y-direction, respectively. Table I presents the data related to the tool and blank finite element meshes.

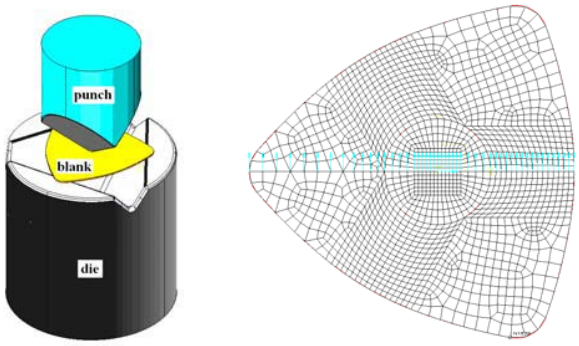

(a) (b)

Fig. 4 (a)The profile of the punch and the die (b)The mesh of blank in orthogonal pressing simulation

TABLE I
TOOL AND BLANK FINITE ELEMENT MESHES

Tool and Blank	Element type	Node number	Element number
Punch	Triangle	1192	2313
Die	Triangle	1634	3179
Blank	Rectangle	1760	1705

A. Boundary Conditions

In forming a equilateral vertical steel, the blank contacts the punch, holder and die. Therefore, the node contacts the tool or moves away from the tool must be determined. The node is classified as a contact node or a free node. Figure 5 presents the boundary conditions pertaining to the combination of the blank and tool system. The node that does not touch the tool is defined as the free node, and its global coordinates are (X, Y, Z). The node that contacts the tool has local coordinates (ξ, η, ζ), following right-hand rule. Accordingly, Y and η are directed into the paper.

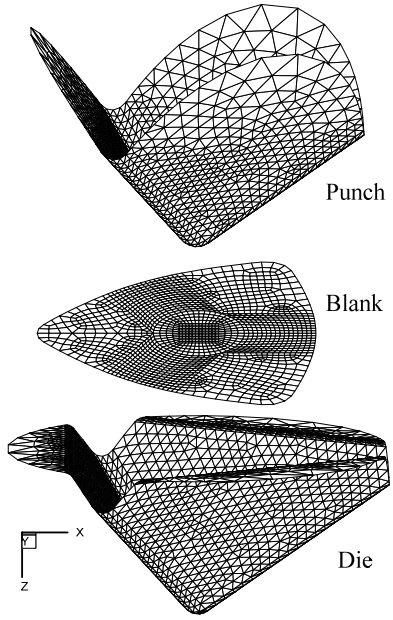

Fig. 5 The mesh of tools are triangular elements and the mesh of the blank is rectangular elements

The contact, or otherwise, made by each node varies with the deformation of the blank. Therefore, during the calculation of the increase in displacement, the normal component of the contacting node force must be checked to determine whether it is less than or equal to zero. The next step in the calculation of the increase in the displacement must be changed; that is, the boundary condition of this node becomes that of a free node. The free node must also be checked to determine whether the contacts the tool. If so, in the subsequent step in the calculation of the increase in displacement, the boundary conditions are changed to those of a contacting node. The above calculation was performed with an extended *r*-minimum.

At the contact interface, the discontinuous alternation between the sliding and sticking states of friction occasionally causes computational difficulty; the treatment of the friction conditions requires special attention. A modified Coulomb friction law, proposed by Oden and Pries [10] and Saran and Wagoner [11], is assumed involving two contact friction states, sticking and sliding; this friction law effectively specifies the discontinuous variation in the direction of sliding . The orthogonal pressing process is simulated by assuming a frictional coefficient of μ =0.05 to describe satisfactory lubrication.

B. Treating the Elastic-Plastic and Contact Problems

The contact condition between the tools and the blank at each node should remain in the same state during incremental

deformation. The *r*-minimum method is applied to elastic-plastic state and extended to treat the tool-metal contact problem [12].

C. Unloading Process

Spring-back or spring-forward is significant in sheet forming; therefore, the unloading behavior following sheet forming is considered. The tools are completely removed at the beginning of the spring-back calculation, and new force boundary conditions are prescribed at all contacted nodes, by setting $\Delta f = -f$.

V. RESULTS AND DISCUSSION

The computation was performed until the punch load increased rapidly when most of the boundary of the sheet came into contact with the tools. Figure 6 presents the relationship between the punch load and punch stroke in the blank of orthogonal pressing processes. The simulated load matches the experimental results for loading; air bending proceeds during the early forming stage in which the punch load varies with the punch stroke, until the bend flange of the sheet touches the face of the die; then, the coining proceeds in the final bending stage in which the punch load increases even more quickly, since most of the boundary of the sheet touches the tools.

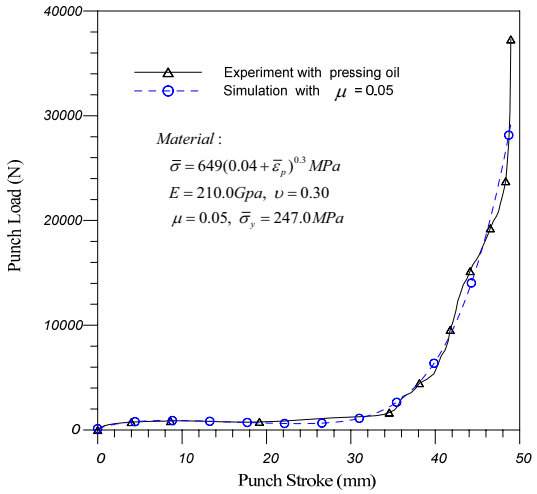

Fig. 6 The punch load-punch stroke relationship

Figure 7 plots the deformed geometries of the square-rail drawing process in the five drawing stages. This figure clearly shows that the sheet was drawn gradually until it enters the unloading state. At the contact interface, penetration, separation and friction throughout the pressing processes were accurately specified by the extended r-minimum method.

Figure 8 shows the von Mises stress distribution for different punch strokes. The stress unit of the color bar is MPa in the picture. When the stroke reaches 25.0 mm, the stress of the orthogonal corner is clearly a maximum. In the final stage, when the stroke is 49.0 mm, the minimum stress is at the arc of outside flange of blank. The greatest stress takes place on the corner of blank, and the corner will be thinning because of increasing in stroke of punch, so the phenomenon of stress concentration is occurred, its value is 638.0MPa. During unloading, the orthogonal workpiece has a large residual stress at the margin of blank.

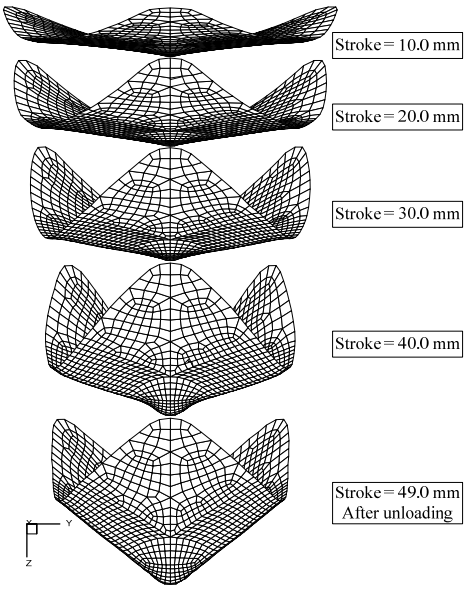

Fig. 7 Schematic representation of orthogonal pressing processes deformed geometry conditions

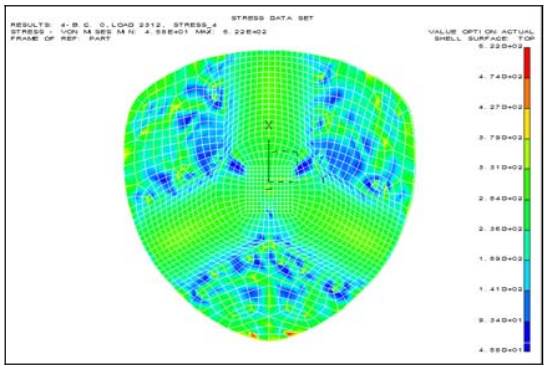

(a) The punch stroke U = 25.0 mm

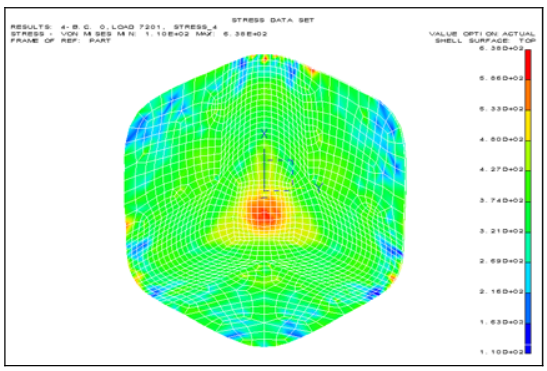

(b) The punch stroke U = 49.0 mm

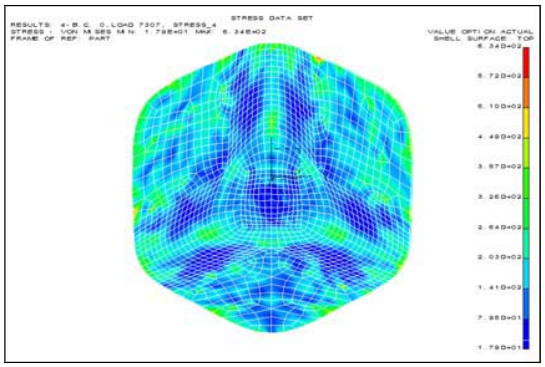

(c) The final shape after unloading

Fig. 8 The distribution of von Mises stress

Figure 9 shows the contours of the principal strain. When the stroke is 25.0 mm, the principal strain of the orthogonal axis is clearly a maximum, because the deformation of orthogonal axis increases as the stroke of the punch, the thickness is thin constantly. In the final step, when the stroke is 49.0 mm, the principal strain is maximum at the orthogonal corner, its value is 0.982. In the unloading step, the principal strain in the orthogonal workpiece remains largest at the orthogonal corner.

Figure 10 plots the reaction force distribution of various strokes. The force unit of the color bar is Newton in the picture. The reaction distribution figure clearly shows the contact between the sheet and the tool. When the stroke is 25.0 mm, the blank contacts the tools like points. When the stroke is 49.0 mm, the sheet totally touches the tools, proving that the pressing processes reach coin step. The maximum of reaction force is $8.75*10^2$ Newton.

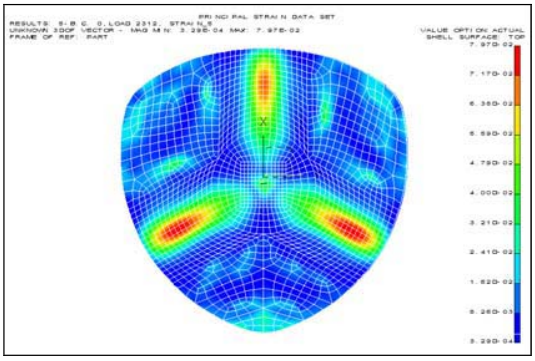

(a) The punch stroke U = 25.0 mm

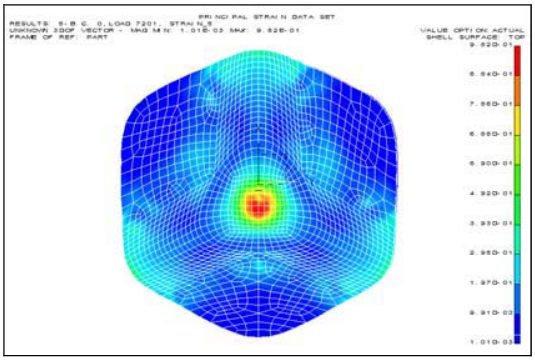

(b) The punch stroke U = 49.0 mm

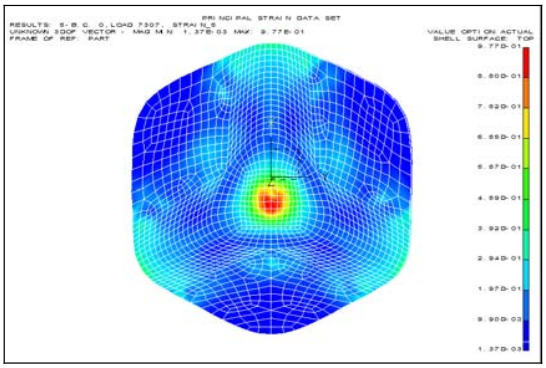

(c) The final shape after unloading

Fig. 9 Show the contour of the principal strain

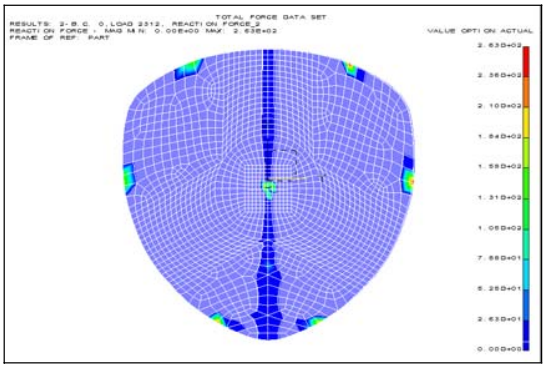

(a) The punch stroke U = 25.0mm

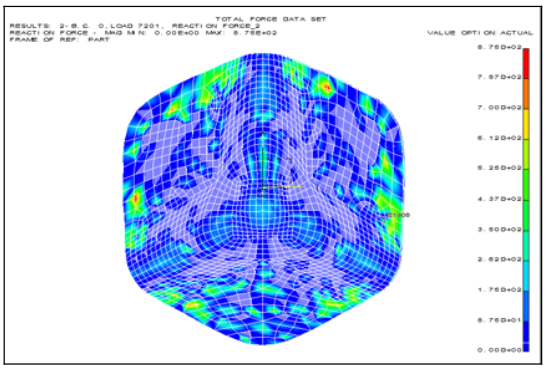

(b) The punch stroke U = 49.0mm

Fig. 10 Reaction force distribution of different strokes.

Figure 11 plots the thickness distribution of final stroke. The thickness unit of the color bar is mm in the picture. The figure shows the thickness distribution during the unloading step. The thickness distribution figure shows that thinnest thickness locates in orthogonal corner. Consequently, if a crack exists, it must be on the orthogonal corner.

VI. CONCLUSIONS

The theoretical computation employed the elasto-plastic large-strain finite-element method with selective reduced integration to develop the simulation program. The large non-linearity of the process was taken into account in an

incremental manner and a *r*-minimum technique was adopted to limit the size of each increment step for a linear relation. The finite-element model yields the following conclusions.

1) Using the finite element method, we analyzed the entire deformation progress of the orthogonal pressing process precisely, implying that the complete history of deformation can be traced successfully.
2) The deformed geometry, the distribution of the stress and strain, and the distribution of thickness are predicted effectively by the finite-element model. This information may be used to improve the manufacturing and design of tools.
3) In orthogonal pressing processes, since the thinnest part of the sheet is on the orthogonal corner, if the crack exists, it must be on the orthogonal corner.
4) Since the tools are depicted using CAD software, the finite-element model can be applied to any arbitrary tool used in the workshop in general pressing processes.

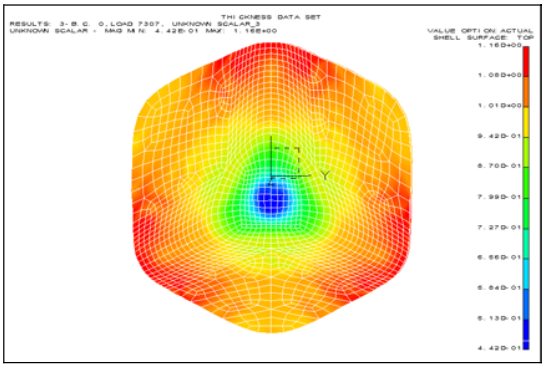

Fig. 11 The thickness distribution

ACKNOWLEDGMENT

The authors would like to thank the National Center for High-performance Computing for computer time and facilities.

REFERENCES

[1] D.S. Malkus and T.J.R. Hughes, "Mixed finite-element methods-reduced and selective integration techniques: a unification of concepts," *Comput. Meth. Appl. Mech. Eng.*, vol. 15(1), 1978, pp.63-81.
[2] R.M. McMeeking and J.R. Rice, "Finite element formulations for problems of large elastic-plastic deformation," *Int. J. Solids Structures*, vol. 11, 1975, pp.601-606.
[3] H.L. Cao and C. Teodosiu, "Finite element calculation of springback effects and residual stress after 2D deep drawing," *Conference proceedings: Computational Plasticity - fundamentals and applications*, Barcelona, Spain, 18-22 September 1989, pp.959-971.
[4] Y. Yamada, N. Yoshimura and T. Sakurai, "Plastic stress-strain matrix and its application for the solution of elastic-plastic problems by the finite element method," *Int. J. of Mech. Sci.*, vol. 10, 1968, pp.343-354.
[5] E. Hinton and D.R. Owen, *Finite Element Software for Plates and Shell*. Pineridge, Swansea, UK, 1984.
[6] T.J.R. Hughes, *The Finite Element Method*. Prentice-Hall, Englewood Cliffs, NJ, 1987.
[7] T.J.R. Hughes, "Generalization of selective integration procedures to anisotropic and nonlinear media," *International Journal of Numerical Methods in Engineering*, vol. 15, 1980, pp.1413-1418.
[8] H.B. Shim and D.Y. Yang, "Elastic-plastic finite element analysis of deep drawing processes by membrane and shell elements," *Journal of Manufacturing Science and Engineering, Transactions of the ASME*, vol. 119, 1997, pp.341-349.
[9] D.K. Leu, T.C. Chen, Y.M. Huang, "Influence of punch shapes on the collar-drawing process of sheet steel," *Journal of Materials Processing Technology*, vol. 88, 1999, pp.134-146.
[10] J.T. Oden and E.B. Pries, "Nonlocal and nonlinear friction law and variational principles for contact problems in elasticity," *Trans. ASME : Journal of Applied Mechanics*, vol. 50, 1983, pp. 67-76.
[11] M.J. Saran and R.H. Wagoner, "A consistent implicit formulation for nonlinear finite element modeling with contact and friction. Part I. Theory,", *Trans. ASME : Journal of Applied Mechanics*, vol. 58, 1991, pp. 499-506.
[12] Y.M. Huang and D.K. Leu, "Finite element analysis of contact problems for a sheet metal bending process," *Int. J. Computers and Structures*, vol. 57, 1996, pp.15-27.